A Comparison of Metrology Used in Documenting Shooting Incident Trajectories

Toby Terpstra[1], Alireza Hashemian[1], Tilo Voitel[2], & Jonathyn Priest[3]

[1]Kineticorp, LLC

[2]Faro Technologies, Inc.

[3]Bevel, Gardner & Associates Inc.

Abstract

There are several methods and tools for documenting trajectory rods, but little research exists comparing accuracies of these methods. In this study, three targets were constructed, each having two sheets of ¼ in (.635 cm) plywood separated by a 3½ in (8.89 cm) void. Three shots from varying locations were taken at each of the targets for a total of nine shots. Prior to each shot, muzzle locations were documented with a total station, and afterwards the bullet hole locations were documented with the total station as well as a 3D laser scanner. Trajectory rods were then inserted through the primary and secondary bullet holes in the plywood targets and aligned using centering cones. This study compares the resulting accuracies from six different methods for documenting the trajectory rods. For each method, the resulting horizontal and vertical trajectory angles were compared to the baseline LiDAR mapping of the bullet holes and muzzle locations. A total of 102 measurements were taken with a combined average horizontal angle accuracy of 1.2° and a standard deviation of 0.9°. The average vertical angle accuracy was 0.7° with a standard deviation of 0.5°.

Keywords: trajectory measurement, laser scanning, LiDAR, photogrammetry, photo scanning, reverse camera projection, shooting reconstruction, crime scene reconstruction, forensic science

Article Information

Received: 22 January 2020
Revised: 7 June 2020
Accepted: 8 September 2020
Published: 11 November 2020

Citation: Terpstra T, Hashemian A, Voitel T, Priest J. A Comparison of Metrology Used in Documenting Shooting Incident Trajectories. *J Assoc Crime Scene Reconstr.* 2020;24:23-42.

Author contact:
tterpstra@kineticorp.com

Introduction

Trajectory rods, also referred to as projection rods, have been an accepted tool for documenting bullet paths in intermediate and terminal targets for many years [1, 2, 3]. Trajectory rods can be used not only in determining shooter position, but also the position and orientation of intermediate targets. The use of trajectory rods, string lines, and laser trajectory pointers makes trajectory measurements possible and create a physical and visual representation of bullet paths and bullet hole locations. This visual information offers insight to initial investigation and serves as a visual tool to all parties involved, including the trier of fact. The utility of trajectory rods for shooting incident reconstruction is evident, but how accurate are these rods for determining bullet path, and what measurement methods are best for documentation? There are several methods and tools for documenting trajectory rods, but little has been done to compare the accuracies of these methods. This study compares six methods for documenting trajectory rods (Table 1).

Testing

Three targets were constructed for this research. Each target was made from two sheets of quarter inch plywood separated by 2×4 framing

Table 1: This table is a summary of methods for trajectory documentation analyzed in this research.

	Method	Type/Tools	Measured
1	Hand Measuring	Zero-edge protractor & inclinometer	Trajectory rods
2	Total Station Mapping	LiDAR (discrete points)	Trajectory rods
3	Laser Trajectory	Laser pointer	Laser path
4	3D scanning	LiDAR (point cloud)	Trajectory spheres
5	Photo Scanning	Pix4D (photogrammetry software)	Trajectory rods
6	Camera Matching Photogrammetry	Reverse camera projection	Trajectory rods

studs. The plywood was painted white and was rigidly affixed to the front and back of the 2×4 posts. Five-gallon buckets, filled with concrete, were used to vertically set and anchor each of the target posts (Figure 1).

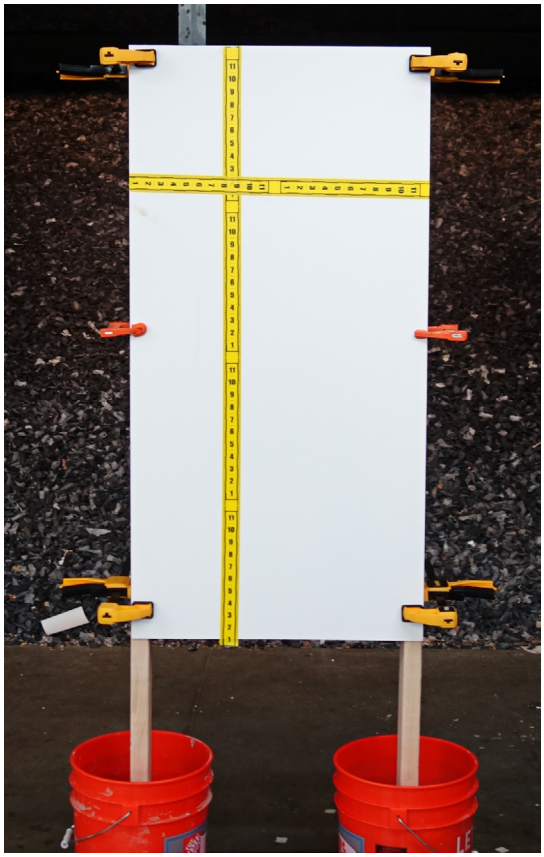

Figure 1: The target setup included 2x4 framing studs anchored in concrete.

The targets were placed within a shooting range and each was mapped using a Sokkia set 530R3 total station and a FARO FocusS350 laser scanner from two locations. This 3D scan data set contained 86.5 million 3D data points commonly referred to as a point cloud. This data set was created prior to shots being fired and did not include trajectory rods. Each target was then shot three times for a total of nine shots. For each of the nine shots, .45 Auto caliber, Federal, 230 grain, full metal jacket (ball) ammunition was fired using a Colt Combat Commander. The velocities of each of the nine shots were recorded using a CED M2 Chronograph. While a true trajectory has a curved path, all shots in this study were taken from less than 50 feet from the targets. At these distances gravitational effects are nominal. The trajectory of a bullet over these distances can generally be considered straight [2] (Table 2).

A Ransom Master Series Handgun Rest was used to eliminate human inconsistencies in the firing process. The shots were fired from a 10-yard (9.14 m) distance line marked at the range. Due to angular differences to the targets, the average distance to target was 35 feet (10.7 m), (Table 2). Prior to each shot, the muzzle location was mapped using the total station, and after the shots were fired, the bullet hole locations were mapped using the total station as well as the 3D scanner. (Figure 2).

The muzzle and bullet hole locations served as the base-line for measuring accuracies of the six methods listed in Table 1. Each of the shots perforated both the front and back of the targets and trajectory rods and centering cones were then placed through the bullet holes (Figure 3).

Measuring Methods

Method 1 – Hand Measuring

Bullet hole locations were measured from the top left corner of each target using a measuring tape. Horizontal and vertical angle measurements were taken for each of the trajectory rods using a zero-edge protractor, manufactured

Table 2: This table shows bullet speed in feet per second and distance to target.

Shot	Speed (ft/s)	Target 1	Target 2	Target 3	Dist. to target	
A	798.4	X			27.3 ft	8.33 m
B	791.5		X		33.9 ft	10.34 m
C	797.8			X	46.6 ft	14.20 m
D	790.8	X			29.4 ft	8.97 m
E	788.2			X	34.8 ft	10.62 m
F	776.2		X		28.0 ft	8.53 m
G	788.6			X	27.8 ft	8.48 m
H	793.2		X		37.0 ft	11.28 m
I	785.9	X			49.3 ft	15.04 m
				Average	**34.9 ft**	**10.64 m**

Figure 2: The testing setup had three targets and was documented using a total station and 3D laser scanning.

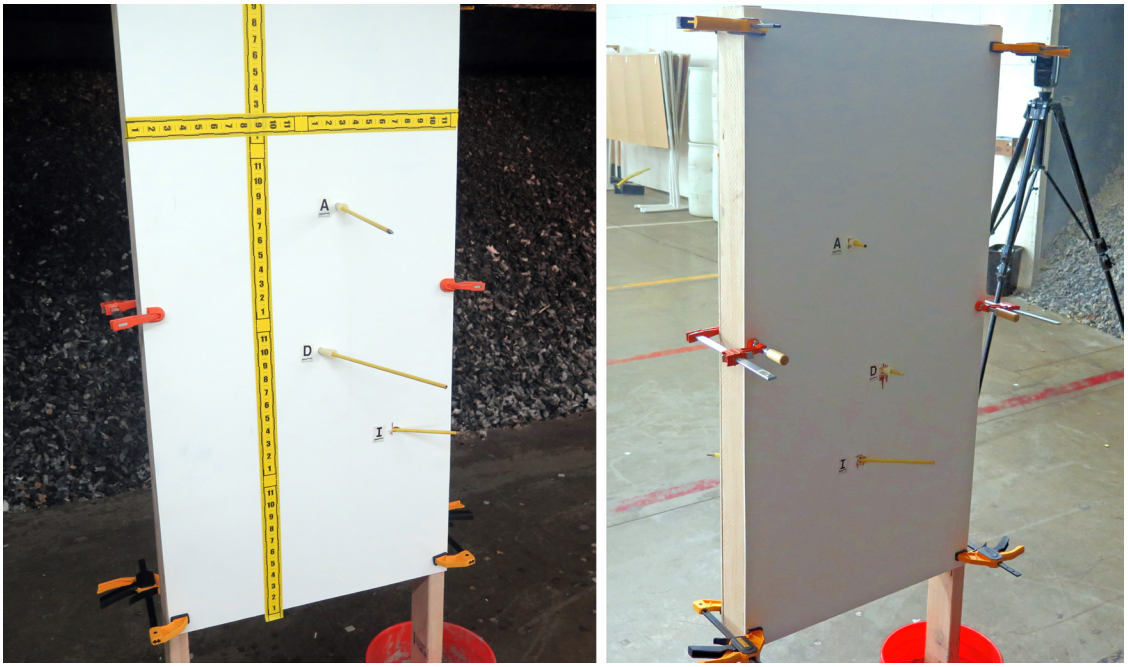

Figure 3: Trajectory rods were placed with centering cones on the front (left) and back (right) of the targets.

Figure 4: Hand measurements were made using a zero-edge protractor and inclinometer (Method 1).

by Loci Forensics B.V., for the horizontal and an inclinometer, manufactured by Johnson, for the vertical (Figure 4). Measurements were written down and then modeled in Autodesk's AutoCAD for comparison to the other methods.

Method 2 – Total Station Mapping

The trajectory rod locations were recorded using a Sokkia set 530R3 reflectorless total station. Two points were mapped on each of the rods to create a trajectory line. The same total station was used in mapping the testing site, the muzzle locations, and the bullet holes. The total station was not moved during the duration of the testing. A backsight check was performed at the end of the scene mapping showing an angular precision of approximately 0.004° (Figure 5).

Method 3 – Laser Trajectory

Laser trajectory mapping was accomplished using a Site Lite SL-500 green laser boresight. It is perhaps more common to affix laser trajectory pointers to the end of trajectory rods, such as those manufactured by Evi-Paq, however this method demonstrates both how a boresight can be utilized and how laser trajectories can be documented using a total station. To accomplish this the boresight (with an aluminum arrow shaft extension) was placed through the bullet holes and aligned using centering cones. With the laser on, a pad of paper was positioned at approximately 12 feet (3.7 m) and 18 feet (5.5 m) from the target such that the green laser was visible. These points were then mapped using the total station (Figure 6).

Figure 5: Total station mapping was completed using a Sokkia set 530R3 reflectorless total station (Method 2).

Figure 6: Laser trajectory mapping was completed using a boresight and mapped using a total station as shown above.

Method 4 – 3D Scanning

The same FARO FocusS350 laser scanner used to document the scene prior to placing trajectory rods, was also used to create a second, separate data set. This second data set included the trajectory rods locations. For this data set, two Koppa 80 mm trajectory spheres were placed on the trajectory rods and secured with O-rings and tape. The Koppa trajectory sphere kit included 12 trajectory spheres such that 6 trajectory rods could be documented without reuse. Due to the limited number of spheres available, three trajectory rods (one on each target) were not documented using this method (Figure 7).

The laser scanner was then used to document the entire site from two scan positions. This resulted in a point cloud with approximately 86.3 million 3D data points. This 3D scan data was then aligned to the baseline survey data in Autodesk AutoCAD 2017. The 3D scan data set alignment was also confirmed in Autodesk 3ds Max 2017. The 80 mm spheres were then created within the modeling software and aligned to the sphere scan data (Figure 8). The sphere alignments were reviewed from multiple angles and verified by colleagues. Lines connecting the center for the modeled target spheres were then used for comparison to the base line survey data (Figure 8).

Method 5 – Photo Scanning

A total of 291 photographs were taken of the targets, the trajectory rods, and the testing site. These were taken for photo scanning purposes and Pix4Dmapper Pro (Version 4.4.4) was used to create a point cloud solution from the photographs (Figure 9).

The point cloud was scaled and aligned

Figure 7: Koppa trajectory target spheres were placed on trajectory rods.

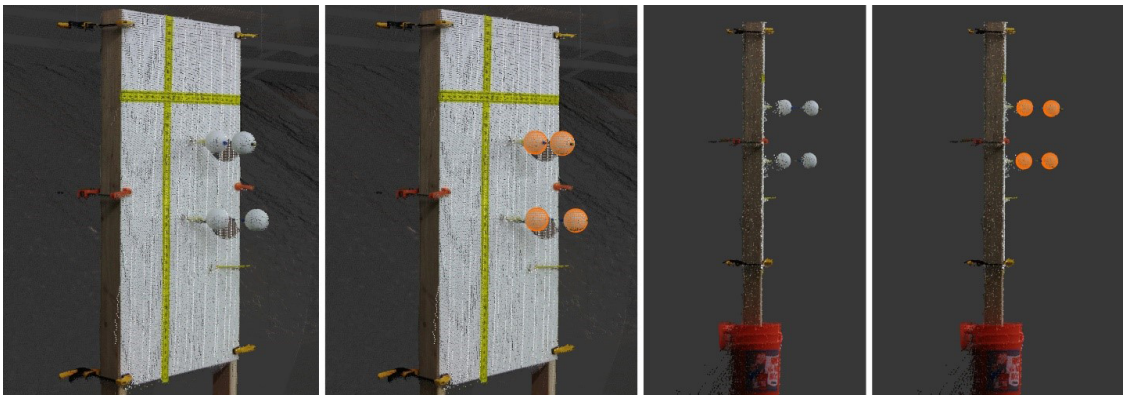

Figure 8: Three-dimensional modeled spheres (orange) were aligned to 3D scan data.

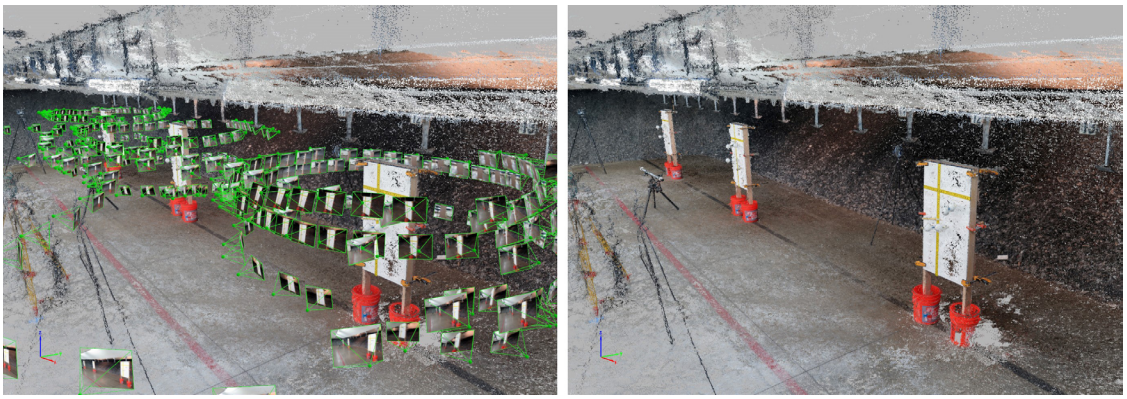

Figure 9: The photo scanning data set is shown with camera solutions (left) and resulting point cloud (right).

within Autodesk 3ds Max. 3D models of the quarter-inch trajectory rods were then aligned to the point cloud and the alignment was verified by colleagues. All three trajectories on all three targets were modeled, including those with scanning spheres, but 3D models of the Koppa target spheres were not created or used for this data set (Figure 10).

A FARO 3D scale bar with a nominal scale of 1,500 mm was setup and scanned during the testing [4]. The photo scan data set was scaled to match the total station mapping and the FARO laser scan data of the testing site. The scale bar was used as further verification of scale.

Method 6 – Camera Matching Photogrammetry

Autodesk 3DS Max was used as the main software for camera matching photogrammetry, but similar methods are possible in other

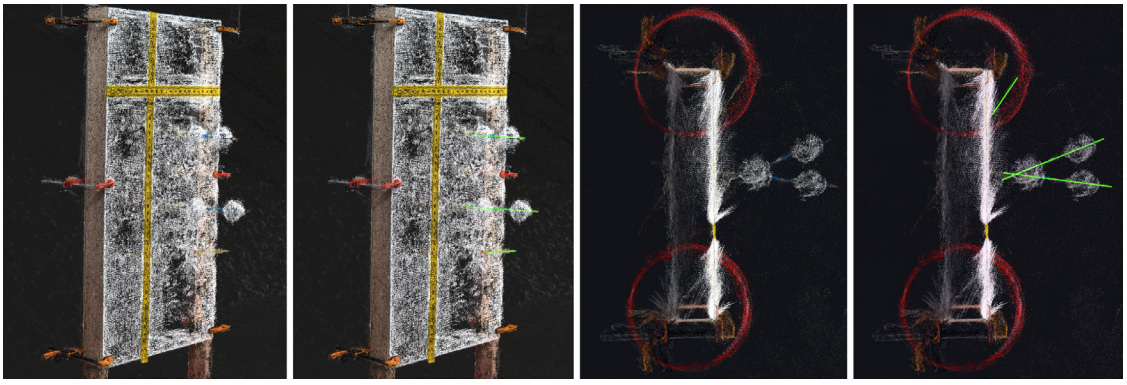

Figure 10: Green modeled trajectory rods were aligned to the photo scan data set as shown in perspective (left) and top (right).

software titles. The scan data used in camera matching was collected prior to the targets being penetrated and did not contain bullet holes, trajectory rods, or scanning spheres. This scan data contained nearly all other scene features that were unchanged between time of scanning and when the photographs with the trajectory rods were taken. This scan data was then imported into the software where a computer-modeled camera was set up to view the model from a perspective that was visually similar to that of the photographs to be analyzed. Three photographs, with differing horizontal and vertical orientations, were selected for each target and analyzed for lens distortion. Lens distortion is an important consideration in any photogrammetric project [5, 6, 7].

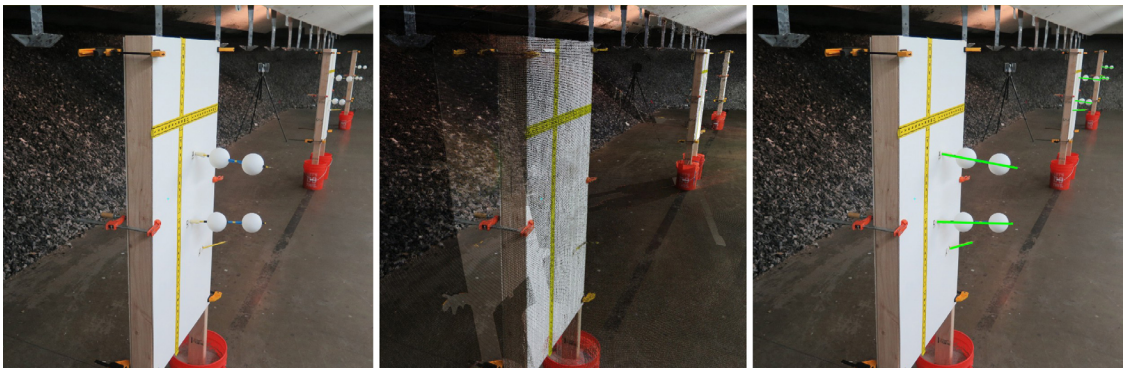

Figure 11: The camera matching photogrammetry solution can be seen with point cloud dada overlaid on photograph (center) & modeled trajectories in green (right).

For purposes of this study, DxO Viewpoint (version 3) was used for lens correction prior to camera matching. The chosen photographs were imported into the modeling software and designated as background images for the computer-modeled cameras. The focal length, field of view, and orientation of the virtual camera was then adjusted until an overlay was achieved between the computer-generated scene model and the geometric features of the scene shown in the photograph. This step yielded a virtual camera representing the location and characteristics of the physical camera. Once the location and characteristics of the camera used to take the photograph were reconstructed, the trajectory rods visible within the photographs were added and aligned to their correct location within the computer environment. Each of the three targets had a photogrammetric solution consisting of at least three photographs (more where multiple targets were visible within a selected photograph). These photogrammetric solutions defined the locations of the trajectory rods such that the computer model locations were consistent with the locations visible within the photographs (Figure 11).

The locations of the modeled trajectory rods were then compared to the baseline. The camera matching photogrammetry process was completed by three photogrammetry experts. Each achieved their own solution which was visually verified by colleagues. The average for all three participants was used for comparison of this methodology. The full data set, with values from each participant, is available in Appendix B.

Results & Conclusions

With trajectories from all six data sets aligned, horizontal and vertical angle differences were measured (Figure 12).

The vertical and horizontal angles for all six methods totaled 102 trajectory angles. These angles were measured against the baseline trajectory angles. The average difference across all six measurement methods was found to be 0.9° with a standard deviation of 0.8° from known trajectory (baseline) angles. Figure 13 shows the average horizontal and vertical angle errors with error bars representing a standard deviation. The full list of angular measurement errors for each method is available in Appendix A.

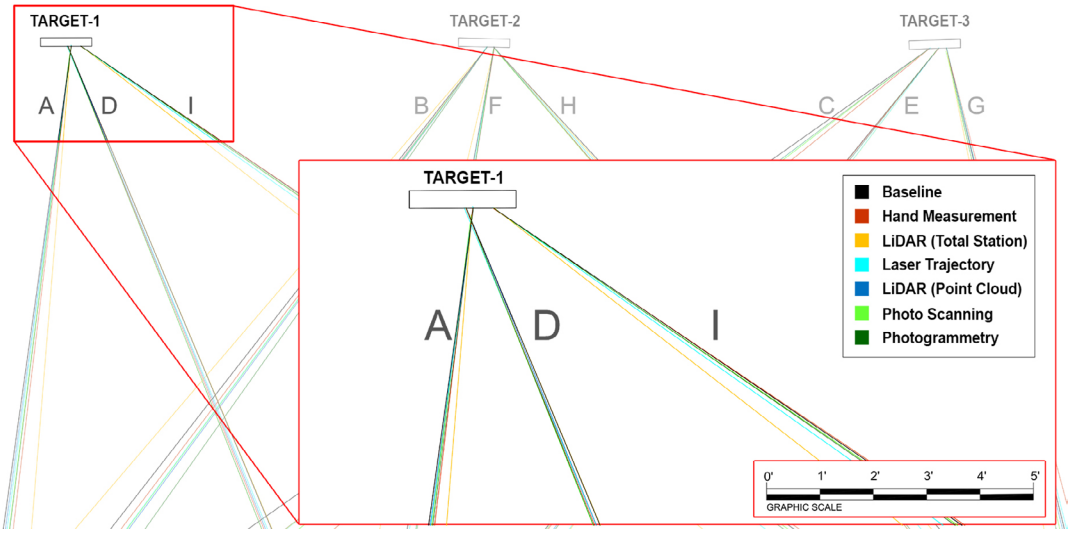

Figure 12: This diagram is a top down view showing the horizontal angles of all six data sets aligned for comparison.

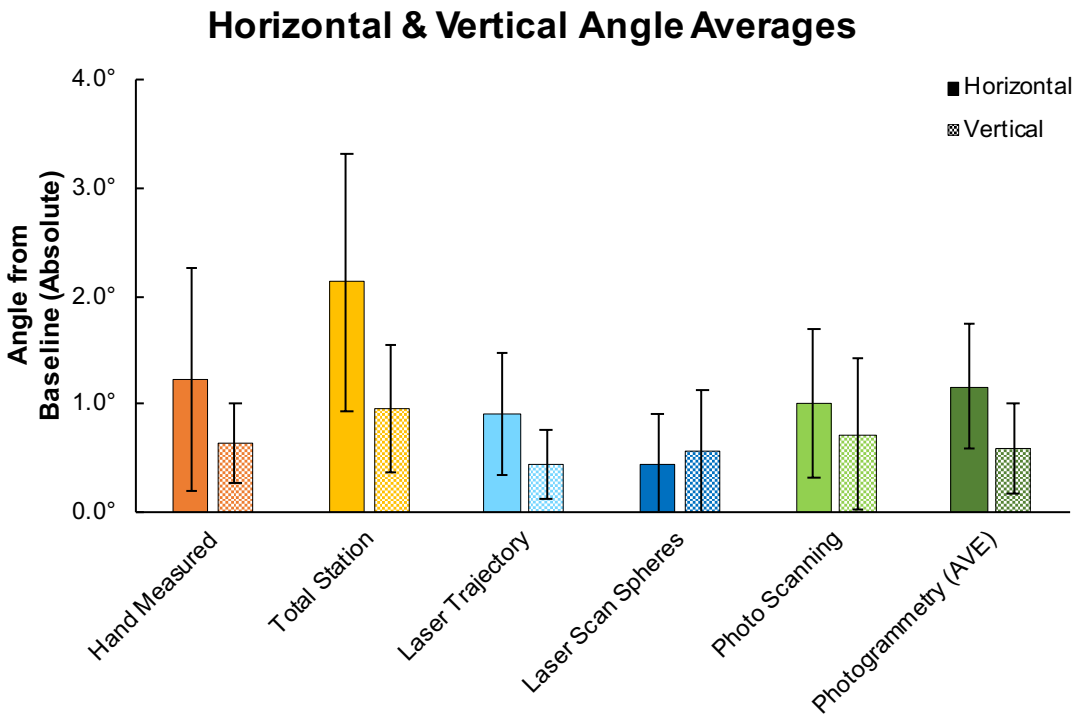

Figure 13: A plot of the average horizontal & vertical angle errors for all 6 mapping methods, with standard deviation error bars.

Method 1 – Hand Measuring

Hand measuring using a zero-edge protractor and inclinometer was found to be an average of 1.2° error in horizontal from the baseline with a standard deviation of 1.0° and 0.6° error in vertical with a standard deviation of 0.4° (Figure 14).

Method 2 – Total Station Mapping

Total station mapping, which recorded reflectorless measurements on the trajectory rods, was found to be an average of 2.1° error in horizontal from the baseline with a standard deviation of 1.2°, and 0.9° error in vertical with a standard deviation of 0.6° (Figure 15).

Method 3 – Laser Trajectory

The laser trajectory method was found to be an average of 0.9° error in horizontal from the baseline, with a standard deviation of 0.6°, and 0.4° error in vertical with a standard deviation of 0.3° (Figure 16).

Method 4 – Laser Scanning

Laser scanning with trajectory spheres was found to be an average of 0.7° error in horizontal from the baseline with a standard deviation of 0.4°, and 0.8° error in vertical with a standard deviation of 0.5° (Figure 17).

Method 5 – Photo Scanning

Photo Scanning was found to be an average of 1.0° error in horizontal from the baseline with a standard deviation of 0.7°, and 0.7° error in vertical with a standard deviation of 0.7° (Figure 18).

Method 6 – Camera Matching Photogrammetry

Camera Matching Photogrammetry was found to be an average of 1.2° error in horizontal from the baseline with a standard deviation of 0.6°, and 0.6° error in vertical with a standard deviation of 0.4° (Figure 19).

Trajectory rod mapping can be accomplished accurately using a minimal number of photographs using camera matching photogrammetry. In this research only three photographs were chosen per target. All three photogrammetry experts achieved similar results, demonstrating both the reliability and accuracy of this method. Camera matching photogrammetry is non-destructive and can be used to verify measurements taken using an alternative method. This method is particularly useful in instances where trajectory rod placements have been photographed but there have been changes to the incident site such that other mapping methods cannot be used.

Rod Placement Error

The resulting errors described in this research contain not only errors in documentation, as is the focus of this paper, but also any errors

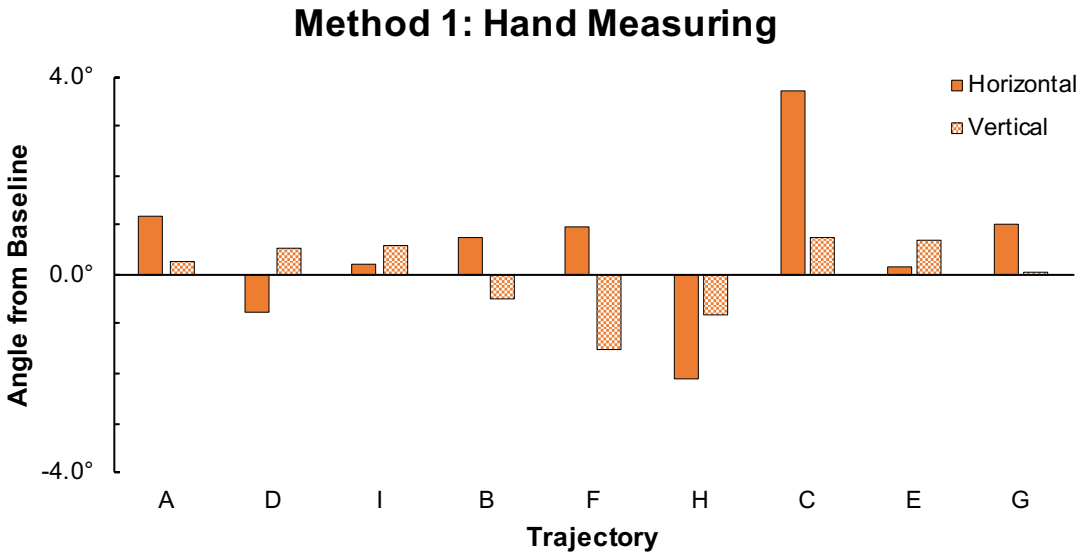

Figure 14: The angular differences from baseline for Method 1 – Hand Measuring.

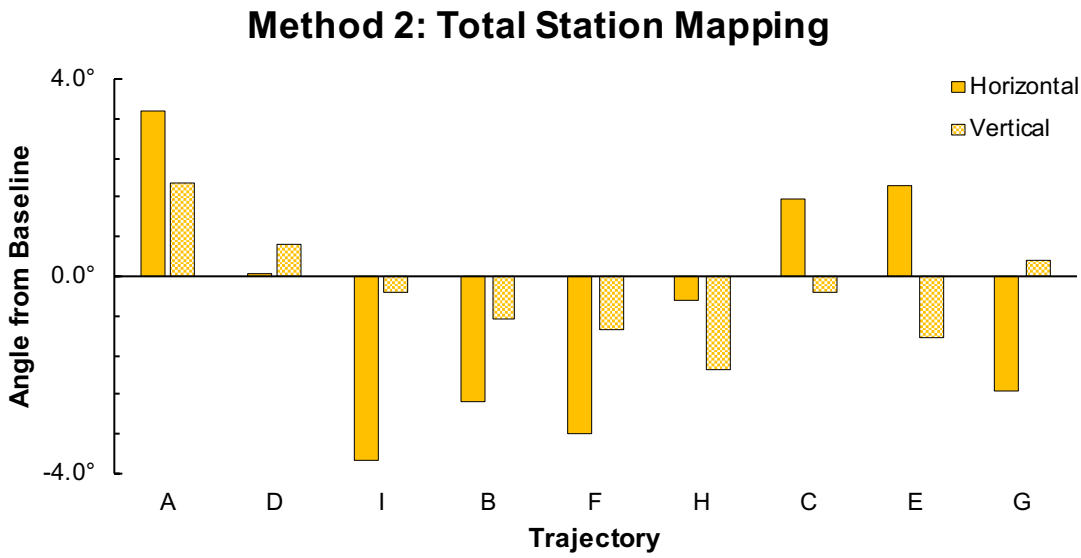

Figure 15: The angular differences from baseline for Method 2 – Total Station Mapping.

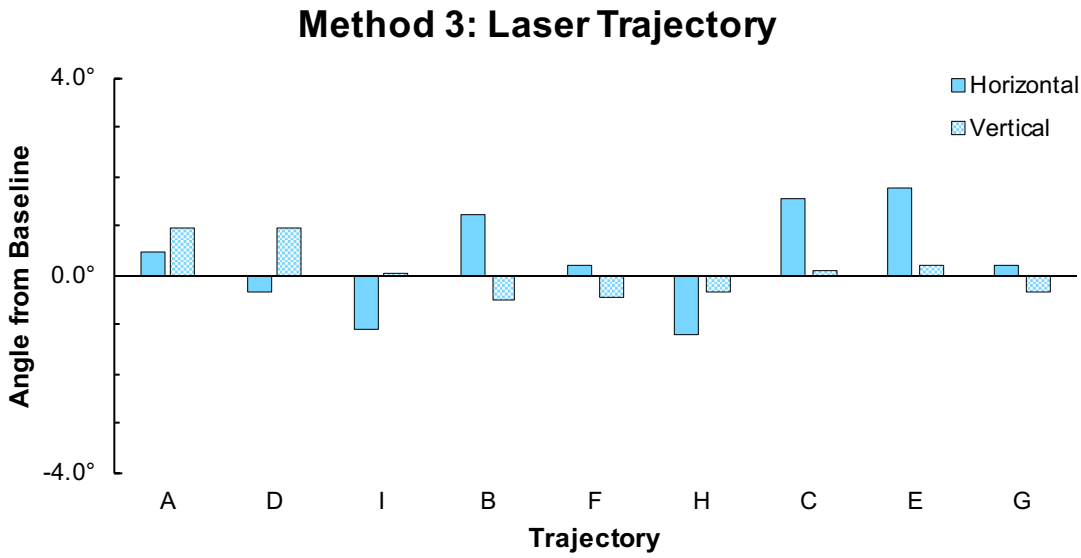

Figure 16: The angular differences from baseline for Method 3 – Laser Trajectory.

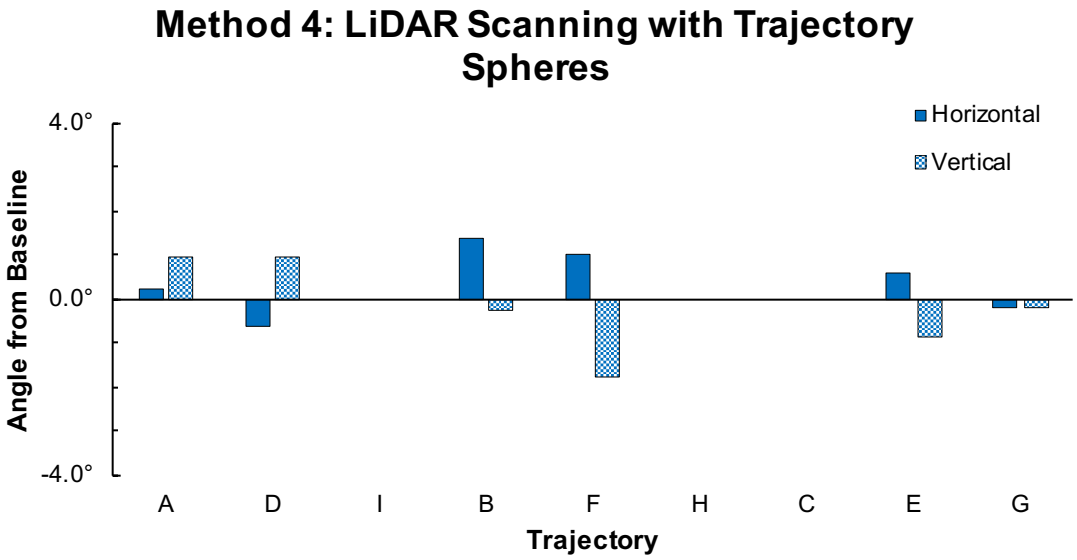

Figure 17: The angular differences from baseline for Method 4 – LiDAR Scanning & Trajectory Spheres.

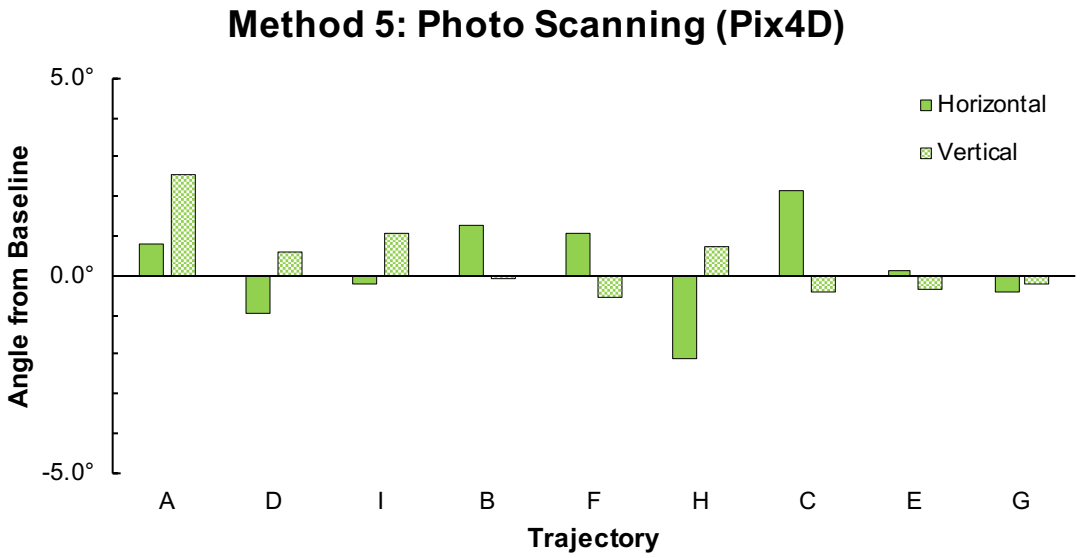

Figure 18: The angular differences from baseline for Method 5 – Photo Scanning.

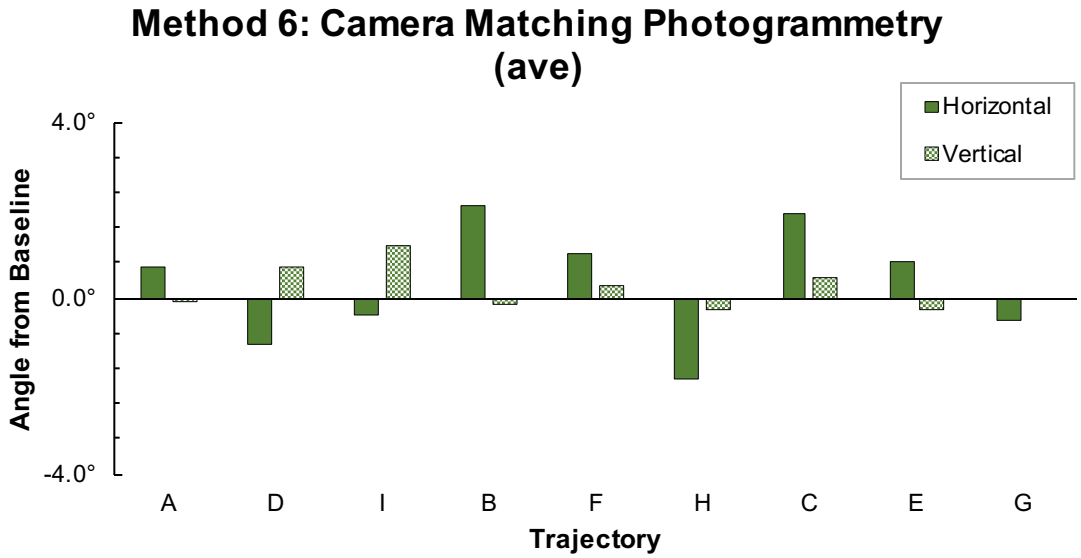

Figure 19: The angular differences from baseline for Method 6 – Camera Matching Photogrammetry.

in rod placement. Determining the amount of error related to the rod placement is outside of the scope of this paper, however a pattern exists in the measured data related to the angle of incidence that indicates some amount of error is a result of the rod placement and not documentation error (Figure 20).

When the horizontal angles for all six of the analyzed methods are plotted together, a general pattern is visible. The majority of data is a positive or negative error depending on the trajectory. For example, all of the measurements for trajectory 'A' are positive errors, and all of the measurements for trajectory 'H' are negative (Figure 21).

The pattern is consistent with the horizontal incidence angles for each trajectory. The average error of each of the nine trajectories (A-G) has a positive value if the angle of incidence was a negative angle, and a negative value if the angle of incidence was positive (Figure 22).

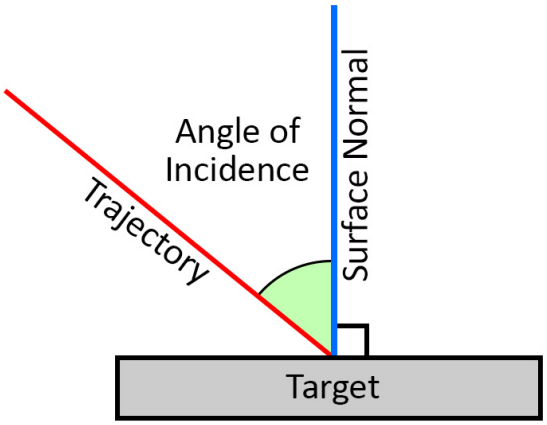

Figure 20: The angle of incidence (green) is measured from the surface normal.

The horizontal trajectories had a minimum incidence angle of -8.2°, a maximum incidence angle of -56.7°, and the average absolute incidence angle was 31.8°. This pattern was not visible in the vertical trajectory angles which were generally more perpendicular to the target and had less variance. The vertical angles had a minimum incidence angle of 0.4°, a maximum incidence angle of -2.6° and the average absolute incidence angle was 1.3°. (Table 3).

This pattern indicates that something in the placement of the trajectory rods with using centering cones into the targets created systematic and predictable error. This error is visible in the measured averages for each horizontal trajectory and has the effect of moving the trajectory rod away from where the shot was fired and towards the target surface normal. It appears that this error is either not present or not as significant in trajectories with a smaller incidence angles such as the vertical angles measured in this research. Quantifying the amount of error related to rod placement and at what incidence angle this error becomes prevalent will require additional study and is outside the scope of this research.

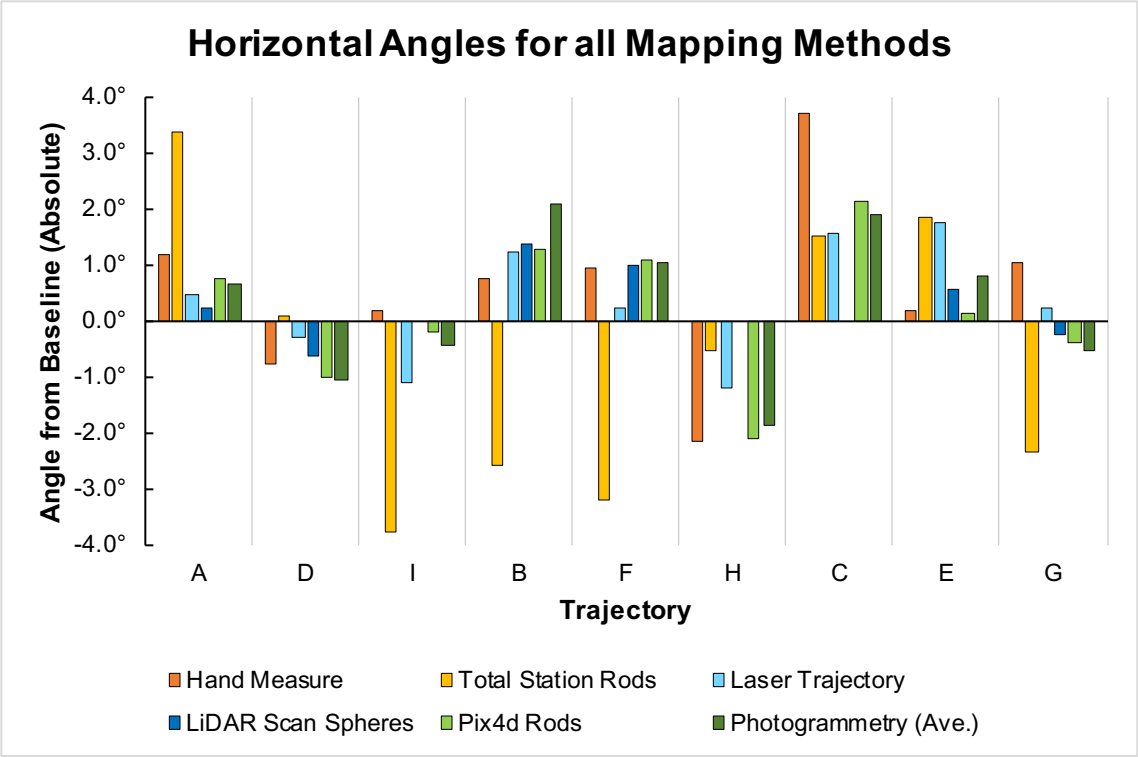

Figure 21: The Horizontal angles for all mapping methods is shown above.

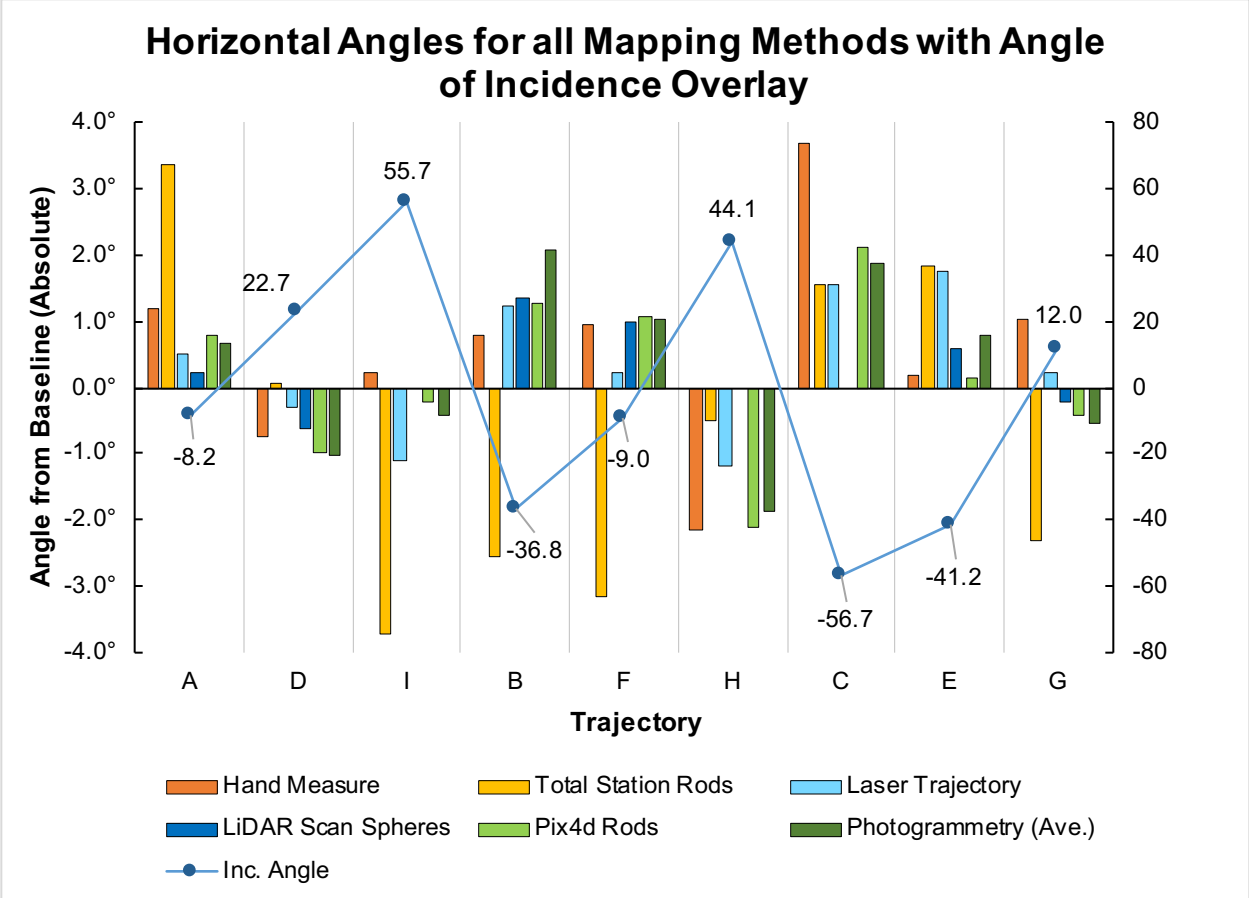

Figure 22: The horizontal angular errors create an inverse pattern with the incidence angles (blue line).

Table 3: The horizontal angle values have an inverted relationship. Negative values are shaded to highlight this pattern.

Horizontal		Error (Ave.)	Inc. Ang.	Inc. Ang. Absolute
Target 1	A	1.1	-8.2	8.2
	D	-0.6	22.8	22.8
	I	-1.0	55.8	55.8
Target 2	B	0.7	-36.8	36.8
	F	0.2	-9.0	9.0
	H	-1.6	44.1	44.1
Target 3	C	2.2	-56.7	56.7
	E	0.9	-41.2	41.2
	G	-0.4	12.0	12.0
			Average	**31.8**

Vertical		Error (Ave.)	Inc. Ang.	Inc. Ang. Absolute
Target 1	A	1.1	-2.3	2.3
	D	0.7	-0.6	0.6
	I	0.5	0.7	0.7
Target 2	B	-0.4	-0.7	0.7
	F	-0.8	-2.6	2.6
	H	-0.5	0.4	0.4
Target 3	C	0.1	-1.3	1.3
	E	-0.3	-0.9	0.9
	G	-0.1	-2.5	2.5
			Average	**1.3**

Discussion

Method 1: Hand measurements

Hand measurements using a zero-edge protractor and an inclinometer is a widely used method for recording trajectories. The hand measuring technique is effective and does not require expensive equipment or software to accomplish. This method however, does require a specific skillset that is best developed through experience. For purposes of this research the measurements were taken by a professional shooting incident reconstructionist. The measurements were recorded by hand and then translated into 3D modeling software. While photographs can be misleading due to perspective, the hand measuring method can be supplemented with a plumb-bob to help eliminate misreading angles within photographs. With hand measurements, photographs can be a good method for recording the data and eliminate the potential for error when translating hand measurements [2].

Method 2: Total station mapping

Total station mapping has been referred to as a simple and accurate method for documenting trajectories [3]. Indeed, the total station was used in creating the baseline data for this research. For this method, the Sokkia set 530R3 total station was used in reflectorless mode, and the lateral or sides of the trajectory rods were mapped. The total station mapping of the trajectories in this research achieved the least accurate results across all six methods. While the results were not expected by the authors, it brings to light the potential for errors when using this method. Total station mapping records discrete points using LiDAR technology. During the total station mapping it was noted that recording two points on the rods that had a trajectory more perpendicular to the total station was easier to accomplish than mapping two points on the rods that pointed more towards the location of the total station. This angle of incidence, or the angle the recording surface is at in relation to the total station position, can play a role in mapping. In this research, the total station was not moved and had a location in the middle of the shooting area. As a result, many of the trajectory rods pointed back near the general location of the total station, creating a less than ideal horizontal incidence angle for recording points. Additionally, the trajectory rods only protruded a short distance out of the front of the targets, leaving a limited area for two total station measurements to be taken to establish the trajectory. In this study the average horizontal incidence angle was 52° and the distance between recorded points on the trajectory rods was 5.7" (19.1 cm) (Table 4).

A small distance error such as 0.1" (2.54 mm) on one of the measurements would create a 1.0° error over a distance of 5.7" (19.1 cm). With a rod thickness of .25" (6.35 mm) a LiDAR point taken by the total station lower or higher on the rod could account for this error (Figure 23).

The authors believe a preferable method for

Table 4: Horizontal incidence angles were not ideal for mapping trajectories with the total station.

Horizontal		Total Station Angle Error	Incidence Angle	Length Between Points
Target 1	A	3.4	18.0	8.9
	D	0.1	45.5	5.4
	I	-3.7	75.9	3.4
Target 2	B	-2.6	13.2	4.8
	F	-3.2	41.9	5.4
	H	-0.5	81.2	5.3
Target 3	C	1.5	82.5	5.3
	E	1.9	80.3	7.5
	G	-2.3	29.6	5.4
		2.12	**52.0**	**5.7**

documenting trajectory rods with a total station is to map the bullet hole location using a fiducial sticker or similar centered over the bullet hole. Then after placing the trajectory rod the end of the rod would be mapped in a similar fashion [3]. Provided that the total station can be setup an adequate distance from the target, this process ensures that the recorded surfaces are more perpendicular to the total station. LiDAR mapping is also known to be less accurate on objects that are shiny and on objects that are reflective. If limitations of space require that the lateral surface or side of the trajectory rod is to be mapped, 3D scanning spray, can be used to reduce the shininess of the rod. While additional research is needed to quantify improved accuracies, following these suggested best practices will help to achieve more reliably and the accuracy that this technology is capable of.

Method 3: Laser trajectories

Laser trajectories offer a straight-line visualization of the bullet path. There are many ways of incorporating laser pointers or laser trajectories to map bullet paths. This research utilized a Site Lite SL-500 green laser boresight with an aluminum arrow shaft extension, allowing the use of centering cones. Other trajectory lasers have threaded mounts and are capable of mounting directly to the end of trajectory rods. Trajectory lasers offer the ability to extend trajectories over longer distances while at the shooting site. Laser trajectories can be photographed using a variety of methods including spray fog, misting water, and moving a white card along the laser path during a long exposure. These photographs can be a useful aid in understanding shooting incidents [8].

Method 4: Laser scanning

Laser scanning uses LiDAR technology and

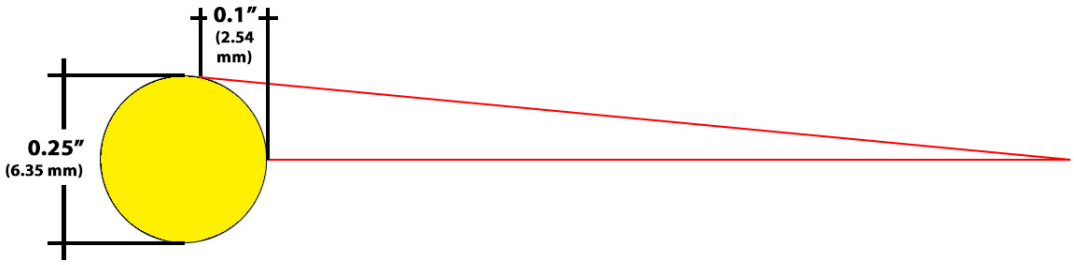

Figure 23: Recording one of the points higher or lower than one centered on the rod, can result in a distance error of 0.1″ (2.54 mm) and an angular error of 1.0°.

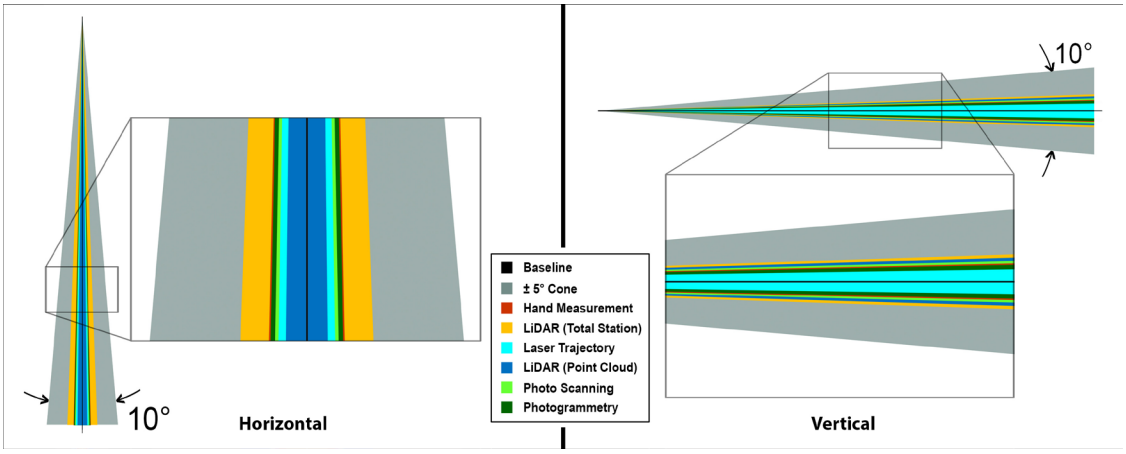

Figure 24: The horizontal (top) and vertical (side) measurement averages for all methods compared to a 5° cone.

is an excellent tool for evidence preservation. 3D scanning offers the ability to document an incident site with millions of 3D data points while simultaneously collecting scan data on trajectory spheres as well as the trajectory rods. Previous research has shown little difference in accuracies resulting from scanning of trajectory rods or trajectory spheres [9]. While the 3D scanner used in this research was a FARO FocusS350, there are several laser scanner manufactures with products on the market. Some of these scanners offer the capability of capturing the entire scene as a 360° scan and then focusing in on a smaller section of the scene where a high-density scan can be performed. Increasing the scan quality settings and the density of points collected on the trajectory spheres and rod surfaces may offer an advantage over lower scan density and may be particularly helpful when trajectory spheres are not used. The scanner was set at ¼ resolution and at 4x quality for a scan duration of approximately 10 minutes. Only two scans were done with the trajectory spheres in place.

Method 5: Photoscanning

Photoscanning, also referred to as multi-view photogrammetry [10], is accomplished by having a series of photographs with enough overlap such that computer software can find similar features for alignment. After aligning the photographs and solving for camera locations, the software is capable of creating a point cloud consisting of a large number of individual 3D points. There are many contemporary photoscanning software titles available with comparable requirements and results [11]. Drone photography and aerial mapping has accelerated this technology and it has expanded into many industries. While having enough photographs with sufficient overlap to create a sufficient point cloud typically takes planning, photoscanning can also be used as a method for rebuilding evidence from a scene or object where the scene has been altered or the object has not been preserved for physical inspection. For this reason, photo scanning can be referred to as both a documentation method and a method for rebuilding a three-dimensional model of the scene.

Method 6: Camera matching photogrammetry

Camera matching photogrammetry has been used in a number of disciplines and is sometimes referred to as reverse camera projection [12, 13]. Similar to photoscanning, camera matching can be used as both a documentation method and a method for rebuilding a three-dimensional model of the scene. Camera matching photogrammetry is capable of delivering highly accurate results with a limited number of photographs [14, 15]. This is especially useful in situations where there is a limited number of photographs and a lack of access for physical examination.

Range of certainty

A ±5° range of certainty has been commonly accepted in shooting incident reconstruction [2, 16, 17]. This research included varying target entrance angles and six methods of

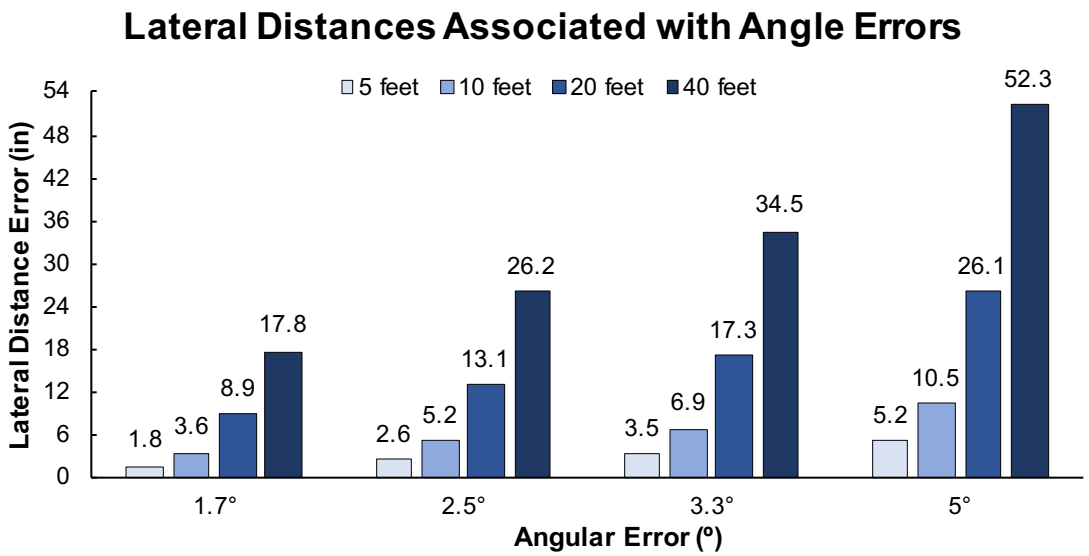

Figure 25: The lateral distance errors are represented as error in one direction (positive). The full range of error would include these distances as both positive and negative.

documentation but was limited to a single weapon and ammunition combination, as well as a single target material type. All 102 trajectory measurements in this study, across all six methods of documentation, fell within the commonly accepted ±5° range of certainty (Appendix A, B). While some methods performed better than others, the average for all angular measurements was 0.9° from the baseline with a standard deviation of 0.8°. This equates to 1.7° at one standard deviation (68%), 2.5° at two standard deviations (95%) and 3.3° at three standard deviations (99.7%). The angular differences measured in this study can be compared visually to the commonly accepted ±5° range or 10° cone (Figure 24).

Using the average for all angular measurements of 0.9° from the baseline with a standard deviation of 0.8°, data representing the standard deviations can be represented graphically over both shorter and longer distances than the shots were fired in the study. Accounting for 68% of the data (One standard deviation) at 10 feet from the target, a 1.7° error equates to 3.6 inches. Accounting for 95% of the data (Two standard deviations) at 10 feet from the target, a 2.5° error equates to 5.2 inches. Accounting for 99.7% of the data (Three standard deviations) at 10 feet from the target, a 3.3° error equates to 6.9 inches (Figure 25).

Alternative methods

There are other methods that can be used for mapping trajectories, including optical or white light scanning, mounted laser positioning such that light from the positioned laser passes through two bullet holes, onsite photogrammetry and using string lines [2, 3, 13]. These methods are similar in nature but are outside the scope of this research.

Acknowledgements

The authors would like to thank the Denver Police Department for use of the shooting range, Nathan McKelvey from Kineticorp for his assistance with total station mapping, and Eric King from Kineticorp for his assistance with camera matching photogrammetry.

References

1. Gardner RM, Bevel T. 2009. Practical crime scene analysis and reconstruction. Boca Raton: CRC Press.

2. Haag LC, Haag MG. 2011. Shooting incident reconstruction. San Diego (CA): Academic Press.

3. Baxter Jr. E. 2015. Complete crime scene investigation handbook. Boca Raton: CRC Press.

4. FARO. 2016. User Manual for the 3D Scale

Bar. [cited 2020 Jan 4]. Available from: https://knowledge.faro.com/Hardware/3D_Scanners/Focus/User_Manual_for_the_3D_Scale_Bar.

5. Wolfgang H. 2010. Correcting lens distortions in digital photographs. [cited 2020 Jan 4] Available from: https://imagemagick.org/Usage/lens/correcting_lens_distortions.pdf.

6. Neale W, Hessel D, Terpstra, T. 2011. Photogrammetric measurement error associated with lens distortion. SAE Technical Paper 2011-01-0286, doi:10.4271/2011-01-0286.

7. Terpstra T, Miller S, Hashemian A. 2017. An evaluation of two methodologies for lens distortion removal when EXIF data is unavailable. SAE Technical Paper 2017-01-1422. doi:10.4271/2017-01-1422.

8. Vecellio M. 2013. Laser visualization of bullet paths. [cited 2020 Jan 4] Available from: http://www.evidencemagazine.com/index.php?option=com_content&task=view&id=1324&Itemid=49.

9. Liscio E, Guryn H, Stoewner D. 2017. Accuracy and repeatability of trajectory rod measurement using laser scanners. *J Foren Sci*. 63(5), 1506–1515. doi: 10.1111/1556-4029.13719.

10. Luhmann T, Stuart R, Stephen K, Jan B. Close-range photogrammetry and 3D imaging. 2nd ed. Walter De Gruyter GmbH, 2014.

11. Terpstra T, Voitel T, Hashemian A. 2016. A survey of multi-view photogrammetry software for documenting vehicle crush. SAE Technical Paper 2016-01-1475. doi:10.4271/2016-01-1475.

12. Bailey A, Funk J, Lessley D, Sherwood C, Crandall J, Neale W, Rose N. 2018. Validation of a videogrammetry technique for analyzing American football helmet kinematics. *Sports Biomechanics.* 1-23. doi:10.1080/14763141.2018.1513059.

13. Terpstra T, Beier S, Neale W. 2019. The application of augmented reality to reverse camera projection. SAE Technical Paper 2019-01-0424. doi:10.4271/2019-01-0424.

14. Callahan M, et al. Close-range photogrammetry with laser scan point clouds. 2012. SAE Technical Paper 2012-01-0607.

15. Terpstra T, Dickinson J, Hashemian A. 2018. Using multiple photographs and USGS LiDAR to improve photogrammetric accuracy. SAE Technical Paper 2018-01-0516. doi:10.4271/2018-01-0516.

16. Haag M. 2008. The accuracy and precision of trajectory measurement. *AFTE J* 2008;40(2):145–82.

17. Hueske EE. 2016. Bullet trajectory analysis using photographs. [cited 2020 Jan 4] Available from: http://www.evidencemagazine.com/index.php?option=com_content&task=view&id=2157&Itemid=41.

Appendix A

Angular differences for each method from known trajectories (baseline).

		Hand Measured		Total Station		Laser Trajectory	
		Horizontal	**Vertical**	**Horizontal**	**Vertical**	**Horizontal**	**Vertical**
Target 1	Trajectory A	1.20	0.27	3.37	1.89	0.49	0.97
	Trajectory D	-0.75	0.56	0.07	0.62	-0.31	0.96
	Trajectory I	0.21	0.60	-3.74	-0.31	-1.09	0.03
Target 2	Trajectory B	0.78	-0.47	-2.55	-0.88	1.23	-0.52
	Trajectory F	0.95	-1.49	-3.17	-1.06	0.22	-0.46
	Trajectory H	-2.13	-0.81	-0.51	-1.90	-1.20	-0.32
Target 3	Trajectory C	3.70	0.76	1.54	-0.31	1.57	0.09
	Trajectory E	0.18	0.68	1.85	-1.24	1.76	0.19
	Trajectory G	1.03	0.06	-2.32	0.33	0.22	-0.34

		Laser Scan Spheres		Photo Scanning		Photogrammetry (AVE)	
		Horizontal	**Vertical**	**Horizontal**	**Vertical**	**Horizontal**	**Vertical**
Target 1	Trajectory A	0.23	0.97	0.78	2.53	0.68	-0.01
	Trajectory D	-0.63	0.92	-0.98	0.59	-1.04	0.69
	Trajectory I	NA	NA	-0.21	1.05	-0.41	1.18
Target 2	Trajectory B	1.36	-0.28	1.26	-0.02	2.08	-0.16
	Trajectory F	0.99	-1.76	1.08	-0.58	1.02	0.28
	Trajectory H	NA	NA	-2.09	0.73	-1.86	-0.29
Target 3	Trajectory C	NA	NA	2.13	-0.39	1.89	0.47
	Trajectory E	0.58	-0.85	0.14	-0.37	0.80	-0.28
	Trajectory G	-0.22	-0.23	-0.40	-0.22	-0.53	0.00

Appendix B

Angular differences from known trajectories (baseline) for Method 6 – Camera Matching Photogrammetry by participant.

		Photogrammetry (P1)		Photogrammetry (P2)		Photogrammetry (P3)	
		Horizontal	**Vertical**	**Horizontal**	**Vertical**	**Horizontal**	**Vertical**
Target 1	Trajectory A	0.51	0.05	0.54	0.03	1.00	-0.11
	Trajectory D	-0.72	0.59	-1.75	1.14	-0.64	0.35
	Trajectory I	-0.87	1.09	0.11	1.31	-0.48	1.14
Target 2	Trajectory B	1.44	-0.41	1.84	0.53	2.97	-0.61
	Trajectory F	0.45	-0.97	0.59	2.51	2.03	-0.71
	Trajectory H	-2.03	-0.31	-1.92	-0.23	-1.62	-0.32
Target 3	Trajectory C	1.43	0.42	2.23	0.76	2.01	0.22
	Trajectory E	0.78	-0.23	1.08	-0.52	0.53	-0.1
	Trajectory G	0.11	-0.57	-0.34	0.03	-1.37	0.54